Chaetocin induces cell cycle arrest and apoptosis by regulating the ROS-mediated ASK-1/JNK signaling pathways

JINGLIANG HE[1,2*], XIAOXUN CHEN[3*], BOWEI LI[4], WENJIE ZHOU[1], JINFENG XIAO[1], KE HE[1], JINQIAN ZHANG[5] and GUOAN XIANG[1]

[1]Department of General Surgery, Guangdong Second Provincial General Hospital, Guangzhou, Guangdong 510317; [2]Department of Postgraduate Studies, Guangdong Medical University, Zhanjiang, Guangdong 524023; [3]Department of Gastrointestinal Surgery, The Guigang City People's Hospital, Guigang, Guangxi 537100; [4]The Third Clinical Medical College of Southern Medical University; [5]Department of Laboratory Medicine, Guangdong Second Provincial General Hospital, Guangzhou, Guangdong 510317, P.R. China

Received March 5, 2017; Accepted August 7, 2017

DOI: 10.3892/or.2017.5921

Abstract. The present study demonstrated that chaetocin, a natural small-molecule product produced by *Chaetomium* fungal species and a potential anticancer agent, inhibited the viability and invasive ability of the human intrahepatic cholangiocarcinoma cell line CCLP-1 *in vivo* and *in vitro* as revealed by CCK-8 and Transwell invasion assays and mouse xenograft tumor experiments. As determined using flow cytometry and intracellular ROS assays, chaetocin was found to induce cell cycle arrest and oxidative stress, leading to CCLP-1 cell apoptosis. Cell apoptosis can be initiated via different apoptotic signaling pathways under oxidative stress. As determined by western blot analysis, expression levels of the apoptosis signal-regulating kinase 1 (ASK-1) signalosome and its downstream c-Jun N-terminal kinase (JNK) signaling pathway were increased under oxidative stress stimulation. These findings indicate that chaetocin arrests the cell cycle and induces apoptosis by regulating the reactive oxygen species-mediated ASK-1/JNK signaling pathways.

Introduction

Chaetocin, a natural small-molecule product produced by *Chaetomium* fungal species (1), has repeatedly been reported to be a promising anticancer agent over the last several years. It has been reported that chaetocin is an inhibitor of lysine-specific histone methyltransferases (HMTs), which are the key enzymes that mediate epigenetic control of gene expression. Chaetocin is also an inhibitor of the redox enzyme thioredoxin reductase, as it competes with thioredoxin for binding to thioredoxin reductase, and thus induces cellular oxidative stress which can eradicate tumor cells (2). Chaetocin has been shown to inhibit the viability of various types of cancer, including melanoma, ovarian and non-small cell lung cancer (3). However, the effects of chaetocin on human intrahepatic cholangiocarcinoma (ICC) and the related mechanisms have not yet been reported.

Human cholangiocarcinoma is an epithelial cell malignancy arising from varying locations within the biliary system, and is the most common primary malignancy of the biliary tract (4). It can be classified into two major categories: ICC and ductal cholangiocarcinoma. ICC has received increased attention as various studies have shown marked increases in the morbidity and mortality rates of ICC in recent years (5). ICC is characterized by insidious development, late onset of symptoms, high recurrence rates after surgical resection, and limited treatment options for the vast majority of patients. Moreover, many ICC cases are resistant to traditional chemotherapeutics due to the desmoplastic character of the cancer, the complex tumor microenvironment and rich genetic heterogeneity (6,7); this creates further challenges for clinical treatment. Therefore, effective therapeutic strategies for the treatment of ICC with minimal side-effects are urgently required.

Induction of apoptosis is considered to be one of the most effective antitumor strategies. Apoptosis is a type of cell suicide that is regulated by a series of complex signaling pathways. Intrinsic or external stimuli induce apoptosis. Oxidative stress, characterized by high concentrations of intracellular reactive oxygen species (ROS), is reported to be one of the intrinsic inducers of apoptosis (8,9).

ROS, which are mainly produced in the mitochondria, have been reported to induce DNA sequence changes (rearrangements, deletions, mutations and gene amplifications)

Correspondence to: Professor Guoan Xiang, Department of General Surgery, Guangdong Second Provincial General Hospital, 466 Xingang Middle Road, Guangzhou, Guangdong 510317, P.R. China
E-mail: bbqsnowhjl@hotmail.com

Professor Jinqian Zhang, Department of Laboratory Medicine, Guangdong Second Provincial General Hospital, 466 Xingang Middle Road, Guangzhou, Guangdong 510317, P.R. China
E-mail: jingwanghou@163.com

*Contributed equally

Key words: chaetocin, intrahepatic cholangiocarcinoma, cell viability, apoptosis, reactive oxygen species, cell cycle, ASK-1, JNKs

and cell apoptosis (10,11). ROS arrest the cell cycle and activate different apoptotic pathways, including the apoptosis signal-regulating kinase (ASK)/c-Jun N-terminal kinase (JNK) pathways (12-14). Previous findings have revealed that chaetocin increases the level of ROS and induces cell apoptosis (15). ROS, which can be produced in response to various types of cytotoxic stressors, activate ASK-1 directly and, thus, activate JNKs downstream (16). Activated JNKs then directly or indirectly activate apoptotic signaling pathways, and this ultimately results in cell apoptosis (17). In the present study, the effect of chaetocin on human ICC and the associated mechanisms were investigated.

Materials and methods

Cell culture and reagents. The human ICC cell lines TFK-1 and CCLP-1 (acquired from the University of Pittsburgh, Pittsburgh, PA, USA) and RBE and SSP-25 (obtained from Piken University, Japan) were cultured in RPMI-1640 medium (Gibco, Grand Island, NY, USA) containing 10% fetal bovine serum (FBS). A normal human intrahepatic bile duct cell line HIBEC (ScienCell Research Laboratories, San Diego, CA, USA) was cultured in the same way as mentioned above. HuCCT1 cells were cultured in Dulbecco's modified Eagle's medium (DMEM) (HyClone, Logan, UT, USA) containing 10% FBS. All cell lines were supplemented with 100 U/ml of penicillin and 100 μg/ml of streptomycin and cultured at 37˚C with 5% CO_2. The cells were split every 4 days and some of the logarithmically growing cells were used for all experiments as described below. Chaetocin (11076 no. 13156; Cayman Chemical Co., Ann Arbor, MI, USA), SP600125 (no. s1460; Selleck Chemicals, Houston, TX, USA) and *N*-acetyl-L-cysteine (NAC) (no. 194603; MP Biomedicals, Solon, OH, USA) were dissolved in dimethyl sulfoxide for usage.

Cell viability analysis. Cell viability was determined by Cell Counting Kit-8 (CCK-8; Dojindo Laboratories, Kumamoto, Japan). In brief, cells were digested and cultured in 96-well plates ($5x10^3$ cells/well) for 24 h. Then, the cells were placed in fresh medium (10% fetal) with different concentrations of chaetocin (0, 50, 100, 150 and 200 nM) for 24, 48 and 72 h, respectively. After incubation for the above times, we replaced each well with CCK-8 at a final concentration of 10% to co-culture for another 1 h. Cell viability was determined by its optical density (OD) measured at 450 nm of absorbance using a microplate reader (Mithras LB 940; Berthold Technologies, Bad Wildbad, Germany). In some experiments, NAC (5 mM) or SP600125 (50 nM) was used for pretreatment for 1 h before incubation with chaetocin. Cell viability = (trial group OD - blank group OD)/(control group OD - blank group OD) x 100%.

Transwell invasion assay. Cell invasion potential was determined using a Transwell chamber (NY14831; Corning Inc., Corning, New York, NY, USA). CCLP-1 cells ($5x10^4$) in serum-free RPMI-1640 medium with different concentrations of chaetocin (0, 100 or 200 nM) were cultured in the upper chamber, which was coated with Matrigel (356234; Corning Inc.). The bottom chambers contained 600 μl medium with 10% FBS. Following 24 h of incubation at 37˚C with 5% CO_2, the cells were fixed using 4% paraformaldehyde and stained with crystal violet at room temperature for 30 min. The cells that invaded to the bottom side of the membrane were photographed at x100 with a microscope (IX71; Olympus, Tokyo, Japan). After that, the bottom membrane with crystal violet was eluted with 33% acetic acid for 30 min and the OD of the acetic acid was determined at an absorbance rate of 570 nm using a microplate reader.

Wright-Giemsa staining. On 6-well plates, $1.0x10^5$ cells/well were seeded and incubated as described above. Solutions of chaetocin (0, 100 and 200 nM) with 10% serum-medium were added to each well, and then incubated for another 48 h. After being fixed with methanol and washed with phosphate-buffered saline (PBS), the cells, stained with Giemsa staining (Xiangya, China), were observed and photographed using an optical inverted microscope at x200 (IX71; Olympus, Tokyo, Japan).

Flow cytometry. The CCLP-1 cells ($15x10^4$/well) were cultured in a 6-well plate as described above. After co-culturing with chaetocin for 48 h, the cells were harvested, and then treated using an Annexin V-FITC apoptosis detection kit and propidium iodide (PI) (BioLegend, Inc., San Diego, CA, USA) according to the manufacturer's protocol. For cell cycle analysis, the cells were cultured with chaetocin for 24 and 48 h, and then fixed with alcohol at 4˚C. After 12 h of fixation, the cells were stained with PI (GBC BIO™ Technologies, Guangzhou, China). Finally, stained cells were analyzed using flow cytometry with FACSCalibur (Becton-Dickinson, Franklin Lakes, NJ, USA) and FlowJo 7.6.1 software.

Intracellular ROS measurement. The intracellular ROS level was determined using an ROS detection kit (KeyGen Biotech Co., Ltd., Nanjing, China) using 2'-7'-dichlorodihydrofluorescein diacetate (DCFH-DA). In brief, after culturing with chaetocin for 24 h in 6 well-plates, the CCLP-1 cells were washed twice using PBS, and then stained with DCFH-DA in the dark for 30 min. Cells were then washed and resuspended in PBS to detect ROS accumulation by flow cytometry with FACSCalibur and analyzed using FlowJo 7.6.1 software.

Western blot analysis. The CCLP-1 cells were treated with different concentrations of chaetocin for 48 h in the presence or absence of SP600125 or NAC. The cells were harvested, and the total proteins were extracted using the protein extraction kit (KeyGen Biotech Co., Ltd.). The proteins were separated on SDS-polyacrylamide gels and transferred to polyvinylidene fluoride membranes (Millipore, Darmstadt, Germany). Antibodies including phospho-ASK-1, phospho-JNK (Cell Signaling Technology, Beverly, MA, USA), phospho-p53, caspase-3, Bcl-2, GAPDH and α-tubulin (Santa Cruz Biotechnology, Inc., Santa Cruz, CA, USA) were used to detected protein. After being washed, the membranes were incubated with homologous secondary antibody for 1 h. The signals were detected with chemiluminescent substrate and photographed using chemiluminescence immunoassay (Tanon 5200; Tanon Science & Technology Co., Ltd., Shanghai, China).

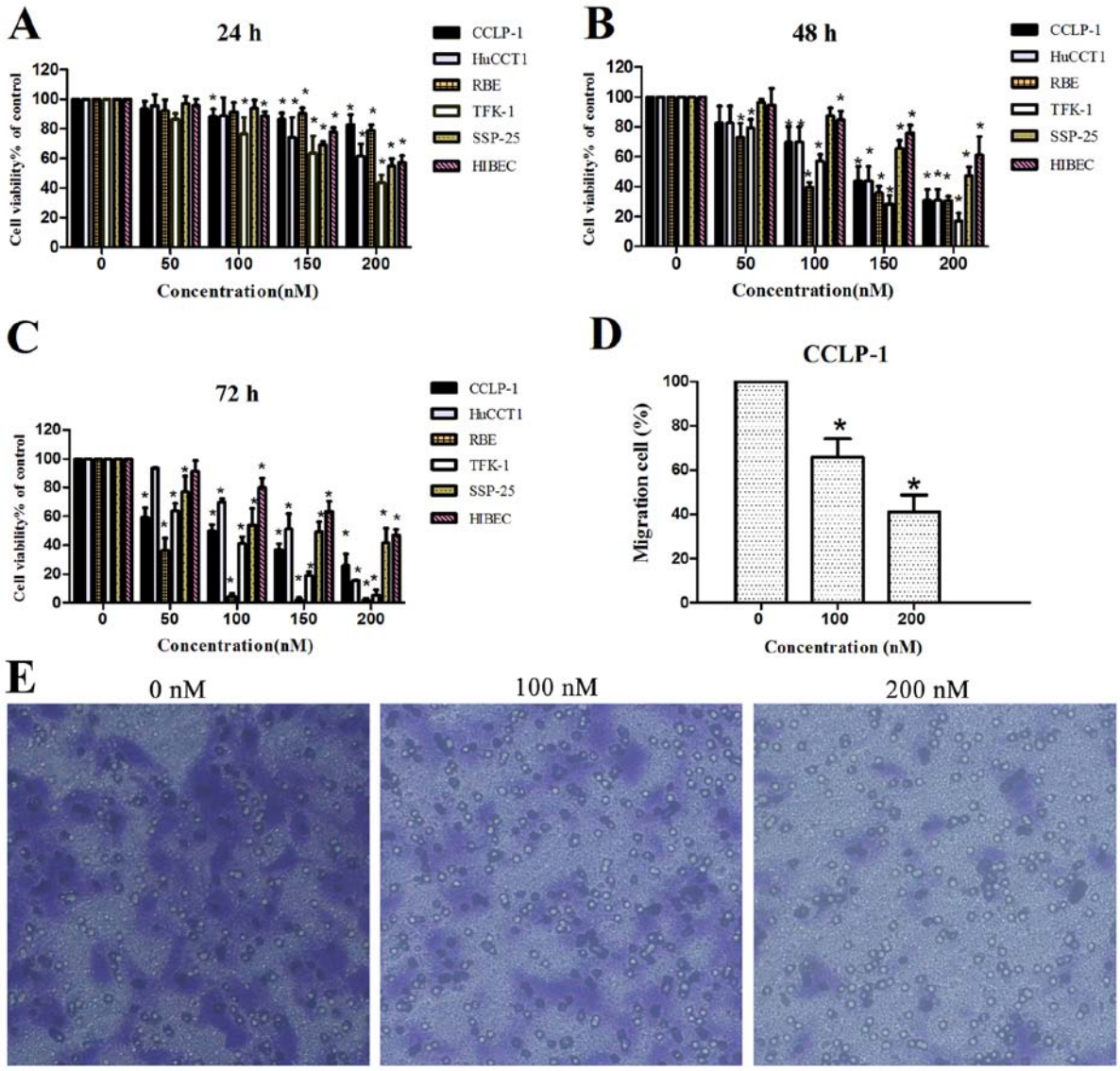

Figure 1. Effects of chaetocin on cell viability and invasion. (A-C) Different ICC cell lines CCLP-1, HuCCT1, RBE, TFK-1 and SSP-25, and normal human intrahepatic bile duct cell line HIBEC were treated with chaetocin at various concentrations (0, 50, 100, 150 and 200 nM) for 24, 48 and 72 h, and then cell viability was detected using CCK-8; *P<0.05 compared with the control group. (D and E) CCLP-1 cells were treated with various concentrations of chaetocin (0, 100 and 200 nM) for 24 h. The cells that invaded to the bottom side of the membrane were observed and photographed at a magnification of x100 via a contrast microscope. Then, the bottom membrane was dyed with crystal violet and eluted with acetic acid and the OD of the acetic acid was detected by a microplate reader; *P<0.05 compared with the control.

In vivo experiment. Twelve nude mice were purchased from the Institute of Laboratory Animal Sciences (Southern Medical University) and used for the xenograft model. The mice were housed in controlled conditions of temperature and humidity with a 12 h light/dark cycle. The experiment was initiated with 6 week-old mice weighing 20-25 g. CCLP-1 cell suspension in PBS ($2x10^6$ cells/ml) was subcutaneously injected into the right flanks of the nude mice. When the mouse tumors reached 3-8 mm in size, the experiment was initiated as the 1st day. Chaetocin was formulated in 3% physiological saline. The nude mice were then randomly divided into 2 groups and were intraperitoneally injected either with chaetocin (0.3 mg/kg body weight) or vehicle once every three days for 6 times and terminated on the 18th day. The tumor dimensions were measured using Vernier calipers once every three days for the entire life span of the mice. Tumor volumes were calculated using the formula: a^2 x $b/2$ (a is the width and b is the length of the tumor in mm). The mice were sacrificed on the 30th day and the tumor mass from each mouse was dissected and weighed. The experimental mice were treated according to the standards supported by the Animal Protection Committee of Southern Medical University.

Statistical analysis. As specified, every experiment was performed at least three times in triplicate, and the results are presented as means ± standard errors (SDs). Statistical analysis was performed by one-way ANOVA or by Student's t-test with SPSS version 18.0 (SPSS, Inc., Chicago, IL, US), and the results were considered statistically significant at P<0.05.

Results

Chaetocin reduces the viability and invasive ability of the ICC cells. In order to investigate the effects of chaetocin on ICC,

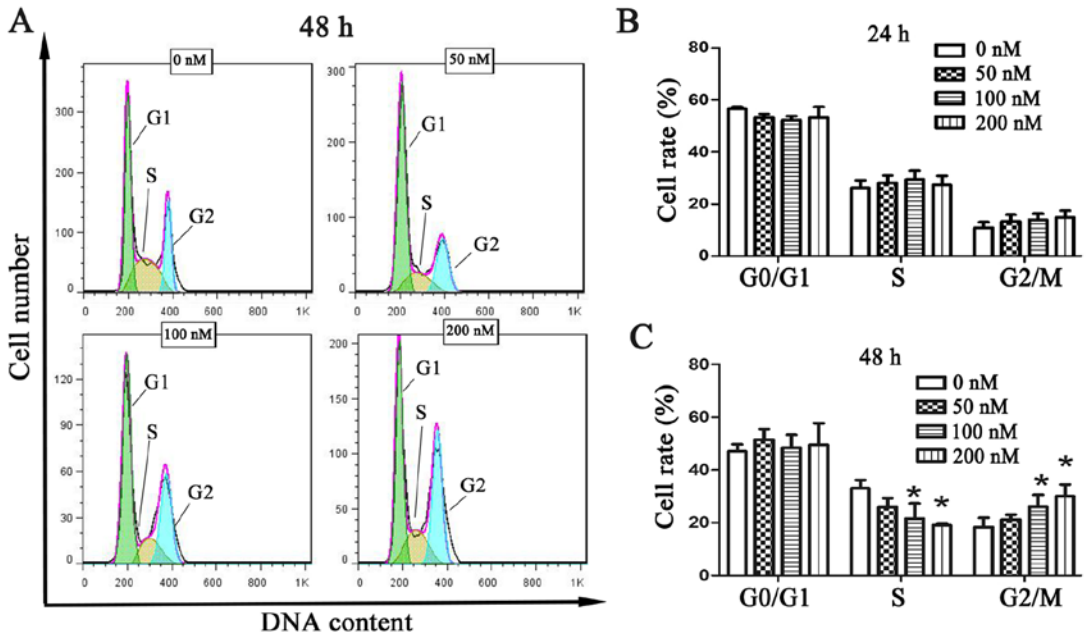

Figure 2. Effects of chaetocin on cell cycle distribution of the CCLP-1 cells. (A) Representative histograms of DNA content in the CCLP-1 cells incubated with chaetocin (0, 50, 100 and 200 nM) for 48 h. (B and C) Histograms display the percentage of cell cycle distribution at 24 or 48 h; $^{*}P<0.05$ compared with the control group.

the viability of different human ICC cell lines was analyzed using a CCK-8 kit, and the invasive ability of the CCLP-1 cells was determined using a Transwell invasion assay. As shown in Fig. 1A-C, chaetocin reduced the viability of all ICC cell lines in a dose- and time-dependent manner. A significant reduction in cell viability was observed when cells were treated with 100 nM chaetocin for 48 h. In addition, the viability of the normal human intrahepatic bile duct HIBEC cell line was reduced in a concentration- and time-dependent manner, but HIBEC sensitivity to chaetocin was lower than that of the cancer cell lines.

Additionally, the invasive ability of the CCLP-1 cell line was reduced by chaetocin. Considering that the reduced ICC viability by chaetocin was significant at 48 h, we decided to observe the results of the Transwell assay after culturing cells with chaetocin for 24 h. Under microscopic observation (magnification, x100), the number of cells that invaded through the membrane in the control group was markedly higher than that in the chaetocin-treated group. Quantification by OD detection confirmed the distinction between the control group and chaetocin-treated group, indicating that chaetocin inhibited the invasion of CCLP-1 cells (Fig. 1D and E).

Chaetocin causes cell cycle arrest in the G2/M phase. To investigate the effect of chaetocin on cell cycle distribution, the cell cycle of CCLP-1 cells was analyzed by flow cytometry, using the PI staining method, following treatment with chaetocin. The results showed that every phase had no statistical difference at 24 h (Fig. 2B). Yet, the number of cells in the S phase was significantly decreased and that in the G2/M phase was increased following chaetocin treatment at 48 h. The changes were statistically significant. These results indicated that chaetocin caused cell cycle arrest in the G2/M phase, inhibiting proper DNA replication (Fig. 2A and C).

Chaetocin induces CCLP-1 cell apoptosis. As the previous experiments revealed, chaetocin exerted an inhibitory effect on ICC cell viability and invasion. We applied Wright-Giemsa staining and flow cytometry was performed to examine whether chaetocin induces CCLP-1 cell apoptosis. Under optical microscopic observation, control group CCLP-1 cells were plump and densely populated in the visual field. However, the cells treated with chaetocin were shriveled and flat with reduced numbers in each visual field. In order to clearly observe the cell morphology, Giemsa was used to stain the cells. Compared with the normal morphology of the control cells, the cells of the chaetocin-treated group exhibited morphological characteristics of apoptosis, including nuclear pyknosis, sublobe, fragmented shapes, fringe collection and apoptotic body formation (Fig. 3A). The number of apoptotic bodies was observably increased with the increasing concentration of chaetocin. To further ascertain the effects of chaetocin on the apoptosis of the CCLP-1 cells, apoptosis was detected using Annexin V-FITC and PI staining. The results (Fig. 3B and C) revealed that the rate of cell apoptosis was increased in a dose-dependent manner, which was more evident at the early apoptotic stage.

Chaetocin induces oxidative stress in the CCLP-1 cells. The intracellular ROS generation in CCLP-1 cells was measured using DCFH-DA. The flow cytometric analysis showed that the chaetocin-treated cells (at high concentrations) had significantly higher levels of ROS than the levels noted in the control cells. However, when cells were cultured with NAC and chaetocin (100 nM), the intracellular ROS level was less than that noted in the chaetocin-treated (100 nM) group (Fig. 4A and C). In addition, a low concentration of chaetocin did not have a significant effect on the ROS level in the cells, which may be the result of the short incubation time. The results suggest

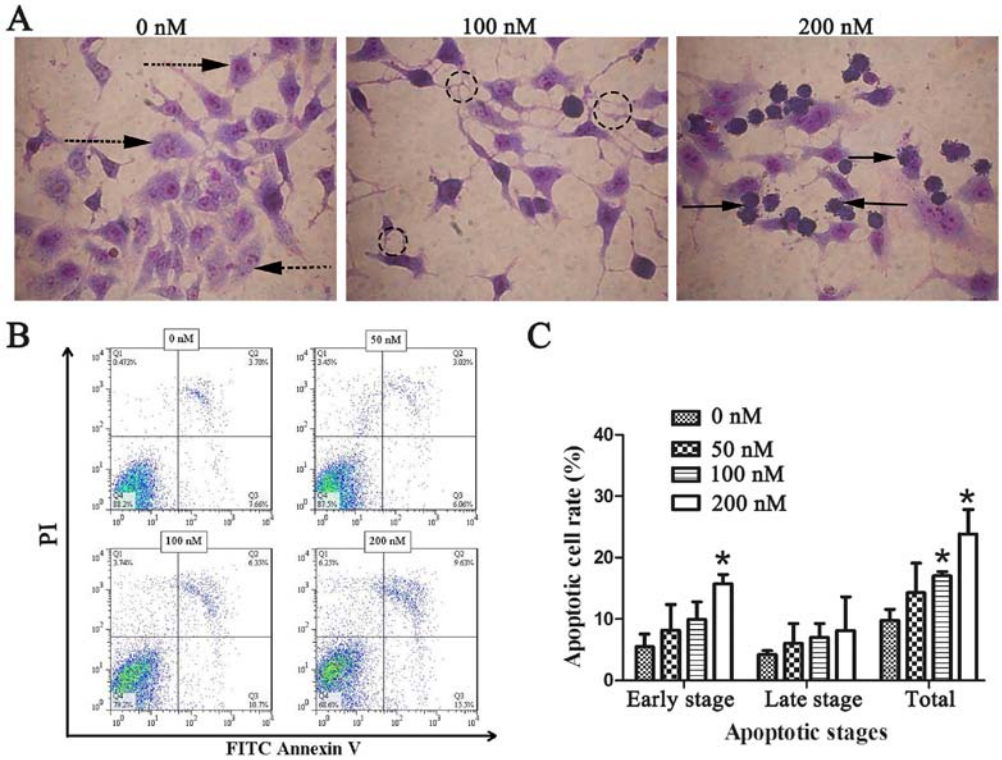

Figure 3. Effects of chaetocin on the apoptosis of CCLP-1 cells. (A) Cell morphology of CCLP-1 cells following treatment with chaetocin (0, 100 and 200 nM) for 48 h and staining with Giemsa and photographed at a magnification of x200 via a contrast microscope. Dotted arrows indicate normal CCLP-1 cells. Dotted circles indicate a change in morphology of the CCLP-1 cells. Solid arrows indicate cell nuclear pyknosis, sublobe, fragment shape (morphological characteristics of apoptosis). (B) The apoptotic ratio of the CCLP-1 cells following treatment with chaetocin (0, 50, 100 and 200 nM) at 48 h was detected using flow cytometry. (C) Histograms display the percentage of apoptotic cells; *P<0.05 compared with the control group.

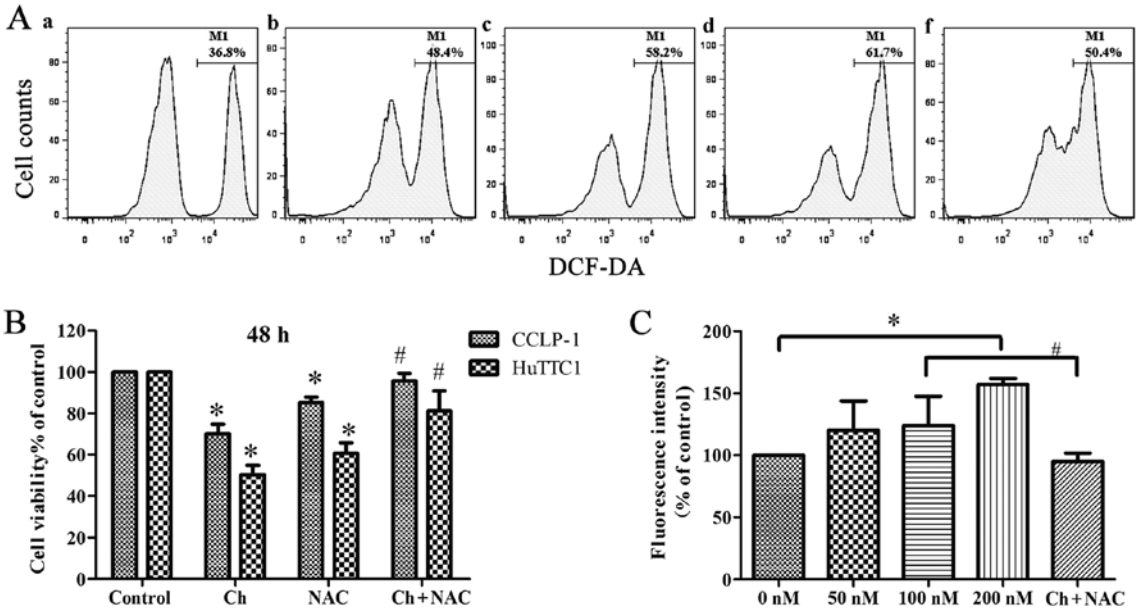

Figure 4. Effect of chaetocin on ROS production in the CCLP-1 cells. (A) The CCLP-1 cells were cultured with chaetocin (0, 50, 100 and 200 nM) (a-d) or 100 nM chaetocin in the present of 5 mM NAC (f) for 24 h. Then, the cells were stained with DCFH-DA and the percentage of DCF fluorescence was detected by flow cytometry. The proportion of cells with bright fluorescence was calculated. (B) The cell lines CCLP-1 and HuCCT1 were cultured with chaetocin (Ch) (100 nM), NAC (5 mM) or both (Ch + NAC) for 48 h, respectively. The viability of the cells was detected via CCK-8; *P<0.05 compared with the control group; #P<0.05 compared with the cells treated with chaetocin. (C) The histograms show the percentage of DCF fluorescence (mean ± SD) compared with the control group; *P<0.05 compared with the control group; #P<0.05, chaetocin (100 nM)-treated group compared with the chaetocin and NAC-treated group.

that chaetocin promotes the generation of intracellular ROS, leading to oxidative stress.

The ASK-1/JNK pathway is involved in CCLP-1 cell apoptosis. ASK-1 is a member of the mitogen-activated protein kinase

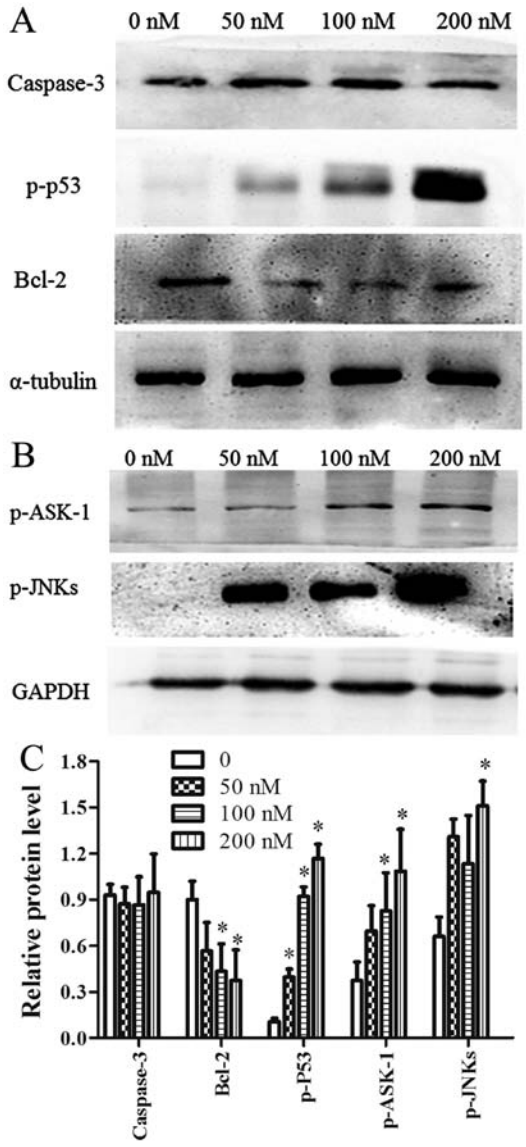

Figure 5. Effect of chaetocin on the protein expression in the CCLP-1 cells. (A-C) Expression changes and relative quantification of proteins were detected by western blotting; 0, 50, 100 and 200 nM are the doses of chaetocin used; *P<0.05 compared with the control group.

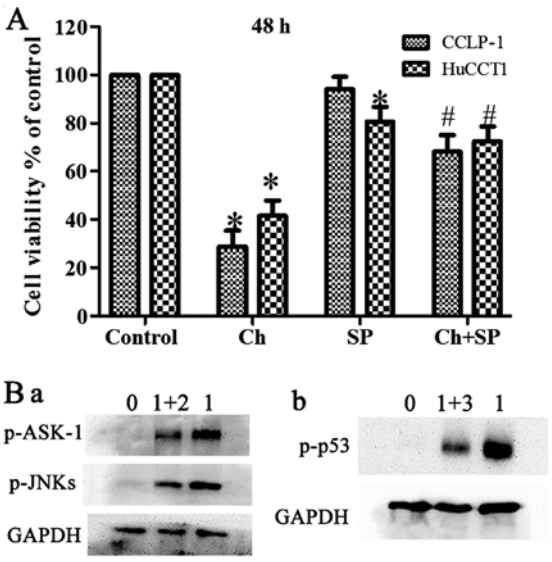

Figure 6. (A) The cell lines CCLP-1 and HuCCT1 were cultured with chaetocin (Ch) (100 nM), SP600125 (50 nM) or both (Ch+SP) for 48 h, respectively. The viability of cells was detected via CCK-8; *P<0.05 compared with the control group; #P<0.05 compared with the cells treated with chaetocin. (B) CCLP-1 cells were treated with chaetocin (100 nM) in the presence or absence of NAC (5 mM) or SP600125 (50 nM) for 48 h. Protein levels of (a) p-ASK-1, p-JNKs and (b) p-p53 were examined by western blotting: 0, control group; 1, chaetocin-treated group; 2, chaetocin-treated and NAC pretreated group; 3, chaetocin and SP600125 treated group.

(MAPK) family that can be activated by oxidative stress. Activated ASK-1 has been reported to activate JNK proteins via phosphorylation. Therefore, the expression of ASK-1/JNK was determined using western blot analysis. The results showed that chaetocin activated ASK-1 and its downstream proteins JNK and p53 in a dose-dependent manner. In addition, the expression level of Bcl-2 was downregulated in a dose-dependent manner. By contrast, following chaetocin treatment, the level of caspase-3 exhibited no obvious change compared with the control (Fig. 5A-C). Furthermore, pretreatment with NAC suppressed the chaetocin-induced activation of ASK-1/JNK, which indicated that ROS have a vital role in the chaetocin-induced activation of these proteins (Fig. 6B-a). In another experiment, pretreatment with SP600125 (a JNK inhibitor) attenuated the chaetocin-induced expression of p53 (Fig. 6B-b).

Chaetocin inhibits the growth of CCLP-1 xenograft tumors in vivo. To detect the antitumor activity of chaetocin *in vivo*, human CCLP-1 cholangiocarcinoma xenografts were established. The results (Fig. 7A-C) showed that the xenografts of the control group grew rapidly, but growth was reduced by chaetocin treatment *in vivo*. Additionally, the average weight of the tumors in the control group was higher than that of the chaetocin-treated group. However, there was no statistically significant difference in tumor weight between the two groups. The difference in tumor weight may have increased if the duration of the experiment had been extended (Fig. 7C). Furthermore, at the time of sacrifice, the average tumor volume of the control group was significantly higher than that of the chaetocin-treated group. Therefore, the results indicated that chaetocin inhibited tumor cell proliferation, although complete regression of the tumor was not observed. Additionally, the average body weight of the chaetocin-treated mice was significantly higher at the beginning of the experiment compared with the weight of the mice at sacrifice. However, this difference was not observed in the control group (Fig. 7D).

Discussion

ICC is a treatment-resistant primary liver cancer with increasing incidence and mortality rates observed worldwide in recent years (18). For the majority of patients with advanced ICC, there is no effective or standard first-line chemotherapy (19). Therefore, it is urgent to identify effective drugs to treat ICC that have minimal side-effects. In our previous preliminary drug screening trials, chaetocin was identified to effectively reduce the viability of RBE cell lines at low doses (20), indicating that chaetocin may effectively inhibit the growth of cancer cells with few side-effects. *In vitro* experiments

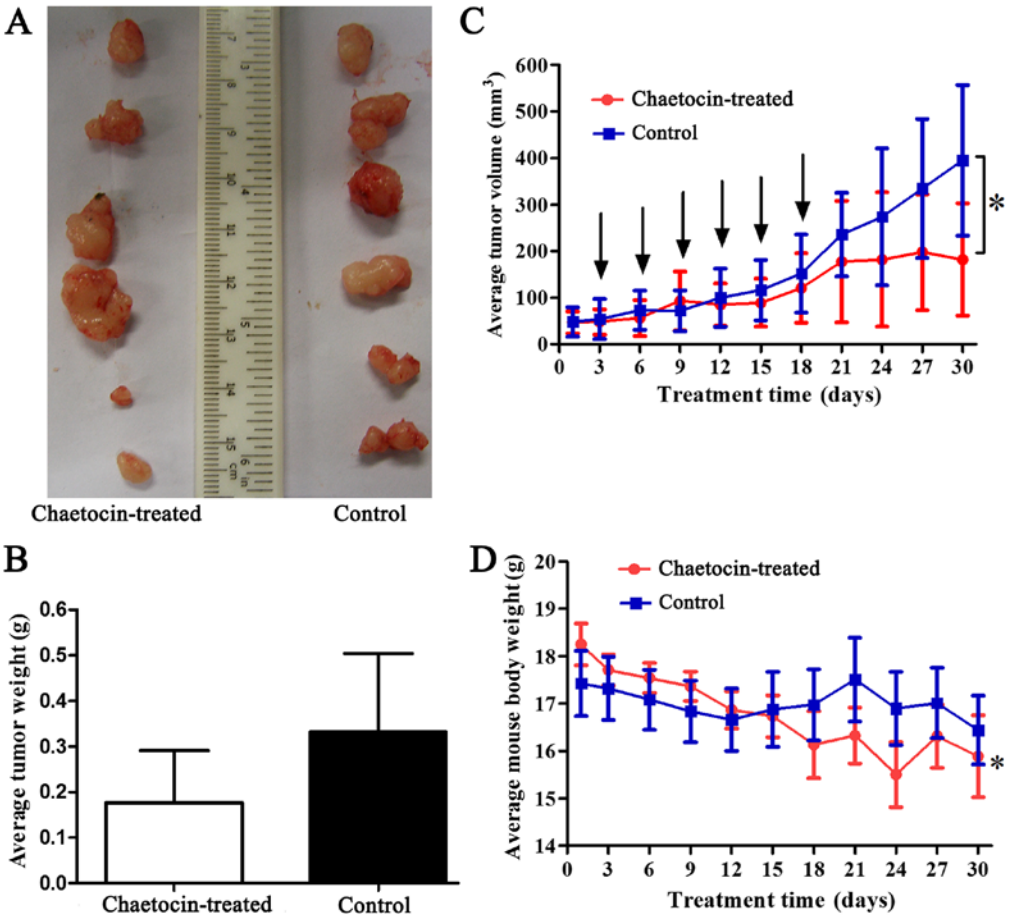

Figure 7. The antitumor effect of chaetocin on xenografts of CCLP-1 *in vivo*. CCLP-1 cells were subcutaneously injected into the rear flanks of nude mice. After the inoculation, mice were randomly grouped and subjected to different treatments as indicated: chaetocin-treated group, intraperitoneally injected with chaetocin (0.3 mg/kg body weight); control group, intraperitoneally injected with vehicle. Mice were sacrificed on the 30th day. (A and B) The image and histograms depict the differences between the two groups in terms of average tumor weight on the 30th day. (C) The curve represents the mean tumor volume/group ± SD (n=6) at different times during the entire experiment. Arrows indicate the times (day) that the mice were injected with either chaetocin or vehicle; *P<0.05, chaetocin-treated group compared with the control group on the 30th day. (D) The curve represents the mean mouse body weight/group ± SD (n=6) at different times during the entire experiment; *P<0.05, weight of initiation compared with weight of termination in the chaetocin-treated group.

in the present study confirmed that chaetocin reduced the viability of ICC cell lines in a dose- and time-dependent manner (Fig. 1A-C). In addition, the Transwell chamber assay demonstrated that chaetocin reduced the invasion of CCLP-1 cells. We hypothesized that chaetocin may have the same effect on other ICC cell lines. Our *in vivo* xenograft tumor model results (Fig. 7A-C) also confirmed that chaetocin inhibited ICC tumor growth in mice. The *in vitro* and *in vivo* experiments clearly showed that chaetocin reduced ICC cell proliferation, but also reduced the viability of HIBECs, a normal human intrahepatic bile duct cell line, although HIBEC cells were less sensitive to chaetocin than the cancer cell lines. *In vivo*, the bdt weight of the mice tended to be decreased following chaetocin treatment. The average body weight change between the early and late stages of the experiment was statistically significant, whereas the body weights of the control group were unchanged (Fig. 7D). Considering these results, the reduced body weight in the chaetocin-treated group may represent a side-effect of chaetocin treatment, which should be noted with due attention. Thus, it is necessary to study the molecular mechanisms that mediate the effects of chaetocin and identify drugs that could be used in combination with chaetocin to potentially reduce the required dose of chaetocin and lessen the associated side-effects.

Cell cycle arrest is a major target of tumor therapy (21). The uncontrolled proliferation of tumor cells is due to overexpression of cyclins or the inactivation of critical cyclin-dependent kinases, which makes tumor cells unable to stop at predetermined points of the cell cycle (22,23). This means that arrest of the cell cycle can inhibit cancer cell proliferation. In the present study, the results showed that every phase in the CCLP-1 cell cycle had no change at 24 h. The results at 48 h showed that the percentage of CCLP-1 cells in the S phase was decreased and that the percentage of cells in the G2/M phase was significantly increased. This indicates that chaetocin was able to arrest the cell cycle in the G2/M phase and decrease DNA replication to inhibit CCLP-1 cell proliferation. Oxidative stress affects the cell cycle by affecting the expression of cyclins (24,25). Considering that the ROS level was not influenced under a low concentration of chaetocin (Fig. 4A), every phase of the cell cycle of the CCLP-1 cells may not have been influenced at 24 h. This assumption requires validation in further experiments.

Apoptosis, a fundamental process essential for the development and maintenance of tissue homeostasis, is also a major

mechanism used to kill cancer cells (26). Inducing apoptosis is now considered as one of the most effective strategies for cancer treatment. In the present study, flow cytometry and observed morphological changes preliminarily indicated that chaetocin induced the apoptosis of CCLP-1 cells (Fig. 3A-C). Additionally, expression of p53 (an executor of apoptosis) was increased by chaetocin (Fig. 5A). This suggests that apoptosis is one of the mechanisms influenced by chaetocin resulting in reduced ICC cell viability.

Considering that pretreatment with NAC partially abrogated the effect of chaetocin on the viability of CCLP-1 cells (Fig. 4B), we aimed to determine whether oxidative stress underlied the chaetocin-induced apoptosis in CCLP-1 cells. ROS, an indicator of oxidative stress, are produced during normal cellular processes and are present in normal and cancer cells. At certain concentrations, ROS are required as critical signaling molecules involved in cell survival and proliferation (27). However, oxidative stress occurs when excessive ROS levels overwhelm the cellular antioxidant system, either through an increase in ROS concentration or a decrease in the cellular antioxidant capacity. Oxidative stress induces cell apoptosis and DNA damage (28,29). The present study showed that the ROS level was higher in the chaetocin-treated group than that in the control group. These results indicate that chaetocin can increase the ROS level and thereby induce oxidative stress in the CCLP-1 cells.

Oxidative stress is an initial signal that can induce cell apoptosis (30). ASK-1 is one of the proteins most sensitive to oxidative stress. It is well known that various types of cytotoxic stressors activate ASK-1 by producing excessive ROS, and thus induce apoptosis (17). Under normal conditions, ASK-1 is inactivated via binding with thioredoxin. ROS can oxidize thioredoxin and dissociate it from ASK-1. Therefore, when oxidative stress occurs, ASK-1 becomes activated via dissociation from thioredoxin and oligomerization into the ASK-1 complex (31,32). The ASK-1 complex phosphorylates itself and induces the activation of JNKs (12,33). JNKs also participate in the regulation of various cellular processes, including cell survival, proliferation, differentiation and cell death (34). A previous study demonstrated that chaetocin inhibited energy production and glucose metabolism in glioma cells in an ROS-JNK-dependent manner (35). Additionally, JNKs are widely reported to have a close association with ASK-1; therefore, we hypothesized that, as JNKs are downstream of ASK-1, they may be involved in the activation of cell apoptosis (36). The potential role of JNKs in chaetocin-induced apoptosis was investigated. As expected, a CCK-8 assay (Fig. 6A) showed that SP600125 (a JNK inhibitor) partially abrogated the effect of chaetocin on ICC cells, and western blotting showed that the chaetocin-induced expression of p53 (a tumor-suppressor gene) was reduced following pretreatment with SP600125 (Fig. 6B-b). Furthermore, in our experiments, the expression levels of phosphorylated ASK-1 and JNKs were increased by chaetocin treatment (Fig. 5A) and decreased by co-treatment with chaetocin and NAC (Fig. 6B-a). This demonstrated that ROS activation of ASK-1/JNK is involved in chaetocin-induced apoptosis of CCLP-1 cells. Following activation of JNKs, apoptosis is mediated by two different signaling pathways: direct and indirect. In the direct pathway, JNKs inhibit Bcl-2, an anti-apoptotic protein, by phosphorylation at Ser-70 (37). In the indirect pathway, JNKs phosphorylate and transactivate other transcription factors, such as p53 (17,38). As expected, our results showed that inhibition of JNKs decreased p53 phosphorylation (Figs. 5A and 6B-b).

In conclusion, chaetocin suppressed ICC cell viability and invasion *in vitro* and tumor growth *in vivo*. Furthermore, chaetocin caused CCLP-1 cell apoptosis, cell cycle arrest and activated the ASK-1/JNK signaling pathways associated with oxidative stress. In addition, chaetocin reduced the viability of a normal bile duct cell line. These results may provide an experimental basis with which to identify new combinatorial drugs that could be used to reduce the required dosage of chaetocin.

Acknowledgements

The present study was supported by grants from the Natural Science Foundation of China (no. 81641110), the Guangdong Province Natural Science Foundation (no. 2015A030313725), and the Guangdong Science Province and Technology Program projects (2012B031800411).

References

1. Isham CR, Tibodeau JD, Jin W, Xu R, Timm MM and Bible KC: Chaetocin: A promising new antimyeloma agent with in vitro and in vivo activity mediated via imposition of oxidative stress. Blood 109: 2579-2588, 2007.
2. Isham CR, Tibodeau JD, Bossou AR, Merchan JR and Bible KC: The anticancer effects of chaetocin are independent of programmed cell death and hypoxia, and are associated with inhibition of endothelial cell proliferation. Br J Cancer 106: 314-323, 2012.
3. Teng Y, Iuchi K, Iwasa E, Fujishiro S, Hamashima Y, Dodo K and Sodeoka M: Unnatural enantiomer of chaetocin shows strong apoptosis-inducing activity through caspase-8/caspase-3 activation. Bioorg Med Chem Lett 20: 5085-5088, 2010.
4. Razumilava N and Gores GJ: Cholangiocarcinoma. Lancet 383: 2168-2179, 2014.
5. Braconi C and Patel T: Cholangiocarcinoma: New insights into disease pathogenesis and biology. Infect Dis Clin North Am 24: 871-884, vii, 2010.
6. Blechacz B, Komuta M, Roskams T and Gores GJ: Clinical diagnosis and staging of cholangiocarcinoma. Nat Rev Gastroenterol Hepatol 8: 512-522, 2011.
7. Sirica AE, Dumur CI, Campbell DJW, Almenara JA, Ogunwobi OO and Dewitt JL: Intrahepatic cholangiocarcinoma progression: Prognostic factors and basic mechanisms. Clin Gastroenterol Hepatol 7 (Suppl): S68-S78, 2009.
8. Flusberg DA and Sorger PK: Surviving apoptosis: Life-death signaling in single cells. Trends Cell Biol 25: 446-458, 2015.
9. Matés JM, Segura JA, Alonso FJ and Márquez J: Oxidative stress in apoptosis and cancer: An update. Arch Toxicol 86: 1649-1665, 2012.
10. Romero A, Ramos E, Ares I, Castellano V, Martínez M, Martínez-Larrañaga M, Anadón A and Martínez M: Oxidative stress and gene expression profiling of cell death pathways in alpha-cypermethrin-treated SH-SY5Y cells. Arch Toxicol 91: 2151-2164, 2017.
11. Zhang Y, Han J, Zhu CC, Tang F, Cui XS, Kim NH and Sun SC: Exposure to HT-2 toxin causes oxidative stress induced apoptosis/autophagy in porcine oocytes. Sci Rep 6: 33904, 2016.
12. Zheng R, You Z, Jia J, Lin S, Han S, Liu A, Long H and Wang S: Curcumin enhances the antitumor effect of ABT-737 via activation of the ROS-ASK1-JNK pathway in hepatocellular carcinoma cells. Mol Med Rep 13: 1570-1576, 2016.
13. Sekine Y, Hatanaka R, Watanabe T, Sono N, Iemura S, Natsume T, Kuranaga E, Miura M, Takeda K and Ichijo H: The Kelch repeat protein KLHDC10 regulates oxidative stress-induced ASK1 activation by suppressing PP5. Mol Cell 48: 692-704, 2012.

14. Kuo PL, Chen CY and Hsu YL: Isoobtusilactone A induces cell cycle arrest and apoptosis through reactive oxygen species/apoptosis signal-regulating kinase 1 signaling pathway in human breast cancer cells. Cancer Res 67: 7406-7420, 2007.
15. Tibodeau JD, Benson LM, Isham CR, Owen WG and Bible KC: The anticancer agent chaetocin is a competitive substrate and inhibitor of thioredoxin reductase. Antioxid Redox Signal 11: 1097-1106, 2009.
16. Tobiume K, Matsuzawa A, Takahashi T, Nishitoh H, Morita K, Takeda K, Minowa O, Miyazono K, Noda T and Ichijo H: ASK1 is required for sustained activations of JNK/p38 MAP kinases and apoptosis. EMBO Rep 2: 222-228, 2001.
17. Sinha K, Das J, Pal PB and Sil PC: Oxidative stress: The mitochondria-dependent and mitochondria-independent pathways of apoptosis. Arch Toxicol 87: 1157-1180, 2013.
18. Xie D, Ren Z, Fan J and Gao Q: Genetic profiling of intrahepatic cholangiocarcinoma and its clinical implication in targeted therapy. Am J Cancer Res 6: 577-586, 2016.
19. Huang Y, Li X and Zhao Y: Progression of targeted therapy in advanced cholangiocarcinoma. Chin J Cancer Res 27: 122-127, 2015.
20. Zhou WJ, Zhang JQ, He K, Duan XP, Huang R, Xia ZL, He JL and Xiang GA: Effects of epigenetic drugs in intrahepatic cholangiocarcinoma cells. Chin J Exp Surg 33: 662-665, 2016.
21. Wiman KG and Zhivotovsky B: Understanding cell cycle and cell death regulation provides novel weapons against human diseases. J Intern Med 281: 483-495, 2017.
22. Liu G, Kuang S and Wu S, Jin W and Sun C: A novel polysaccharide from *Sargassum integerrimum* induces apoptosis in A549 cells and prevents angiogensis in vitro and in vivo. Sci Rep 6: 26722, 2016.
23. Schwartz GK and Shah MA: Targeting the cell cycle: A new approach to cancer therapy. J Clin Oncol 23: 9408-9421, 2005.
24. Pyo CW, Choi JH, Oh SM and Choi SY: Oxidative stress-induced cyclin D1 depletion and its role in cell cycle processing. Biochim Biophys Acta 1830: 5316-5325, 2013.
25. Gao L and Williams JL: Nitric oxide-donating aspirin induces G_2/M phase cell cycle arrest in human cancer cells by regulating phase transition proteins. Int J Oncol 41: 325-330, 2012.
26. Li S, Dong P, Wang J, Zhang J, Gu J, Wu X, Wu W, Fei X, Zhang Z, Wang Y, *et al*: Icariin, a natural flavonol glycoside, induces apoptosis in human hepatoma SMMC-7721 cells via a ROS/JNK-dependent mitochondrial pathway. Cancer Lett 298: 222-230, 2010.
27. Ray PD, Huang BW and Tsuji Y: Reactive oxygen species (ROS) homeostasis and redox regulation in cellular signaling. Cell Signal 24: 981-990, 2012.
28. Duan Y, Gao Y, Zhang J, Chen Y, Jiang Y, Ji J, Zhang J, Chen X, Yang Q, Su L, *et al*: Mitochondrial aldehyde dehydrogenase 2 protects gastric mucosa cells against DNA damage caused by oxidative stress. Free Radic Biol Med 93: 165-176, 2016.
29. Fan XY, Chen XY, Liu YJ, Zhong HM, Jiang FL and Liu Y: Oxidative stress-mediated intrinsic apoptosis in human promyelocytic leukemia HL-60 cells induced by organic arsenicals. Sci Rep 6: 29865, 2016.
30. Kwon YH, Bishayee K, Rahman A, Hong JS, Lim SS and Huh SO: *Morus alba* accumulates reactive oxygen species to initiate apoptosis via FOXO-caspase 3-dependent pathway in neuroblastoma cells. Mol Cells 38: 630-637, 2015.
31. Hayakawa R, Hayakawa T, Takeda K and Ichijo H: Therapeutic targets in the ASK1-dependent stress signaling pathways. Proc Jpn Acad Ser B Phys Biol Sci 88: 434-453, 2012.
32. Madan E, Gogna R, Kuppusamy P, Bhatt M, Mahdi AA and Pati U: SCO2 induces p53-mediated apoptosis by Thr^{845} phosphorylation of ASK-1 and dissociation of the ASK-1-Trx complex. Mol Cell Biol 33: 1285-1302, 2013.
33. Tobiume K1, Matsuzawa A, Takahashi T, Nishitoh H, Morita K, Takeda K, Minowa O, Miyazono K, Noda T and Ichijo H: ASK1 is required for sustained activations of JNK/p38 MAP kinases and apoptosis. EMBO Rep 2: 222-228, 2001.
34. Ki YW, Park JH, Lee JE, Shin IC and Koh HC: JNK and p38 MAPK regulate oxidative stress and the inflammatory response in chlorpyrifos-induced apoptosis. Toxicol Lett 218: 235-245, 2013.
35. Dixit D, Ghildiyal R, Anto NP and Sen E: Chaetocin-induced ROS-mediated apoptosis involves ATM-YAP1 axis and JNK-dependent inhibition of glucose metabolism. Cell Death Dis 5: e1212, 2014.
36. Mantzaris MD, Bellou S, Skiada V, Kitsati N, Fotsis T and Galaris D: Intracellular labile iron determines H_2O_2-induced apoptotic signaling via sustained activation of ASK1/JNK-p38 axis. Free Radic Biol Med 97: 454-465, 2016.
37. Kelkel M, Cerella C, Mack F, Schneider T, Jacob C, Schumacher M, Dicato M and Diederich M: ROS-independent JNK activation and multisite phosphorylation of Bcl-2 link diallyl tetrasulfide-induced mitotic arrest to apoptosis. Carcinogenesis 33: 2162-2171, 2012.
38. Shi Y, Nikulenkov F, Zawacka-Pankau J, Li H, Gabdoulline R, Xu J, Eriksson S, Hedström E, Issaeva N, Kel A, *et al*: ROS-dependent activation of JNK converts p53 into an efficient inhibitor of oncogenes leading to robust apoptosis. Cell Death Differ 21: 612-623, 2014.